UCSF
UC San Francisco Previously Published Works

Title
PON2 subverts metabolic gatekeeper functions in B cells to promote leukemogenesis

Permalink
https://escholarship.org/uc/item/7nd4r2wp

Journal
Proceedings of the National Academy of Sciences of the United States of America, 118(7)

ISSN
0027-8424

Authors
Pan, Lili
Hong, Chao
Chan, Lai N
et al.

Publication Date
2021-02-16

DOI
10.1073/pnas.2016553118

Peer reviewed

eScholarship.org Powered by the California Digital Library
University of California

PON2 subverts metabolic gatekeeper functions in B cells to promote leukemogenesis

Lili Pan[a,b,1], Chao Hong[c,1,2], Lai N. Chan[a,1,3], Gang Xiao[d], Parmanand Malvi[e], Mark E. Robinson[a], Huimin Geng[c], Srinivasa T. Reddy[f], Jaewoong Lee[a], Vishal Khairnar[d], Kadriye Nehir Cosgun[a], Liang Xu[d], Kohei Kume[a], Teresa Sadras[d], Shaoyuan Wang[b], Narendra Wajapeyee[e], and Markus Müschen[a,g,3]

[a]Center of Molecular and Cellular Oncology, Yale Cancer Center, Yale School of Medicine, New Haven, CT 06511; [b]Department of Hematology, Fujian Provincial Key Laboratory of Hematology, Fujian Institute of Hematology, Fujian Medical University Union Hospital, 350001 Fujian, China; [c]Department of Laboratory Medicine, University of California, San Francisco, CA 94143; [d]Department of Systems Biology, City of Hope Comprehensive Cancer Center, Monrovia, CA 91016; [e]Department of Biochemistry and Molecular Genetics, University of Alabama at Birmingham, Birmingham, AL 32533; [f]Department of Molecular and Medical Pharmacology, David Geffen School of Medicine, University of California, Los Angeles, CA 90095; and [g]Department of Immunobiology, Yale University, New Haven, CT 06511

Edited by Michael Reth, University of Freiburg, Freiburg, Germany, and approved December 1, 2020 (received for review August 4, 2020)

Unlike other cell types, developing B cells undergo multiple rounds of somatic recombination and hypermutation to evolve high-affinity antibodies. Reflecting the high frequency of DNA double-strand breaks, adaptive immune protection by B cells comes with an increased risk of malignant transformation. B lymphoid transcription factors (e.g., IKZF1 and PAX5) serve as metabolic gatekeepers by limiting glucose to levels insufficient to fuel transformation. We here identified aberrant expression of the lactonase PON2 in B cell acute lymphoblastic leukemia (B-ALL) as a mechanism to bypass metabolic gatekeeper functions. Compared to normal pre-B cells, PON2 expression was elevated in patient-derived B-ALL samples and correlated with poor clinical outcomes in pediatric and adult cohorts. Genetic deletion of *Pon2* had no measurable impact on normal B cell development. However, in mouse models for BCR-ABL1 and NRAS^{G12D}-driven B-ALL, deletion of *Pon2* compromised proliferation, colony formation, and leukemia initiation in transplant recipient mice. Compromised leukemogenesis resulted from defective glucose uptake and adenosine triphosphate (ATP) production in *PON2*-deficient murine and human B-ALL cells. Mechanistically, PON2 enabled glucose uptake by releasing the glucose-transporter GLUT1 from its inhibitor stomatin (STOM) and genetic deletion of *STOM* largely rescued *PON2* deficiency. While not required for glucose transport, the PON2 lactonase moiety hydrolyzes the lactone-prodrug 3OC12 to form a cytotoxic intermediate. Mirroring PON2 expression levels in B-ALL, 3OC12 selectively killed patient-derived B-ALL cells but was well tolerated in transplant recipient mice. Hence, while B-ALL cells critically depend on aberrant *PON2* expression to evade metabolic gatekeeper functions, PON2 lactonase activity can be leveraged as synthetic lethality to overcome drug resistance in refractory B-ALL.

B cell leukemia | paraoxonase 2 | glucose transport | lactonase

During early B cell development, B cell precursors undergo multiple rounds of V(D)J recombination of immunoglobulin heavy and light chain genes (1). Genetic lesions during somatic recombination events carry a substantial risk of clonal evolution and leukemogenesis (2, 3). Hence, developing B cells are under intense selective pressure for removal of premalignant cells. As a protective mechanism against transformation, B lymphoid transcription factors (IKZF1 and PAX5) function as metabolic gatekeepers and restrict glucose and energy supply to levels that would not satisfy the energy demands of oncogenic transformation (4–6), while fasting selectively inhibits the development of B cell acute lymphoblastic leukemia (B-ALL) but not myeloid leukemia (7). Based on these observations, one would predict that oversupply of glucose and energy will subvert metabolic gatekeeper functions enforced by the B lymphoid transcription program. Several lines of evidence suggest that high abundance of glucose and energy supply in the context of obesity and diabetes indeed increases the risk of B-ALL relapse after initially successful therapy (8–11). These clinical observations suggest a role of increased glucose and energy supply in the etiology of B-ALL and B-ALL relapse.

PON2 is a member of the paraoxonase family of detoxifying (12) and antioxidant enzymes (13). PON2 is localized to the inner mitochondrial membrane and associates with complex III of the electron transport chain (ETC). It binds directly to coenzyme Q10, a cofactor of the ETC and a scavenger of reactive oxygen species (ROS) (14, 15). In response to oxidative stress, PON2 can translocate to the plasma membrane in a manner dependent on intracellular calcium levels (16). Independent of its role in reducing intracellular oxidative stress, PON2 functions as a lactonase to hydrolyze lactone rings. For instance, the bacterial signaling molecule *N*-(3-oxo-dodecanoyl)-L-homoserine lactone (3OC12) is hydrolyzed to 3OC12 acid by PON2 (*SI Appendix*, Fig. S1*A*), causing intracellular acidification (17) and caspase 3/7-dependent apoptosis (18). Interestingly, high expression levels of *PON2* predict poor clinical outcomes in renal and cervical cancers (19). With relevance to human B-ALL, expression of *PON2* has been used as a classifier in different low-density arrays (LDAs) developed to identify high-risk *Ph*-like B-ALL, a subtype characterized by genetic alterations in cytokine receptor and tyrosine kinase signaling (20–23). Analyzing gene expression data from

Significance

B lymphoid transcription factors (e.g., IKZF1 and PAX5) not only mediate B cell lineage commitment but also repress glucose transport and energy supply, thus acting as metabolic gatekeepers. While previous studies showed regulation of metabolic gatekeeper functions at the transcriptional level, we here discovered a mechanism of regulation based on protein–protein interactions between PON2 and the glucose-transport inhibitor stomatin (STOM).

Author contributions: M.M. designed and supervised research; L.P., C.H., L.N.C., G.X., P.M., J.L., V.K., K.N.C., L.X., K.K., and T.S. performed research; S.T.R., S.W., and N.W. contributed new reagents/analytic tools; L.P., C.H., L.N.C., G.X., P.M., M.E.R., H.G., J.L., V.K., K.N.C., L.X., K.K. and T.S. analyzed data; and L.N.C. and M.M. wrote the paper.

The authors declare no competing interest.

This article is a PNAS Direct Submission.

Published under the PNAS license.

See online for related content such as Commentaries.

[1]L.P., C.H., and L.N.C. contributed equally to this work.

[2]Present address: Institutes of Biology and Medical Sciences, Soochow University, 215123 Jiangsu, China.

[3]To whom correspondence may be addressed. Email: lainga.chan@yale.edu or markus.muschen@yale.edu.

This article contains supporting information online at https://www.pnas.org/lookup/suppl/doi:10.1073/pnas.2016553118/-/DCSupplemental.

Published February 2, 2021.

pediatric high-risk B-ALL and adult B-ALL cases, we uncovered that high expression levels of *PON2* predict unfavorable clinical outcomes. While the role and mechanism of action of PON2 in B-ALL remain largely unknown, we here studied a potential role of PON2 in normal B cell development and leukemogenesis. In addition to frequent deletion of *PAX5* and *IKZF1*, we identified aberrant expression of *PON2* as a mechanism to bypass metabolic gatekeeper functions. While B-ALL cells critically depend on PON2 to evade metabolic gatekeeper functions, its lactonase activity can be leveraged for synthetic lethal effects of 3OC12 lactone.

Results

High PON2 mRNA Levels Predict Poor Clinical Outcome in B-ALL Patients. Studying gene expression data from clinical trials for adult (Eastern Cooperative Oncology Group, ECOG E2993) and pediatric (St. Jude Children's Research Hospital) (24) B-ALL cases, we found that *PON2* mRNA levels were significantly higher in Ph^+ B-ALL patient samples in comparison to normal pre-B cells (Fig. 1*A*). Similarly, analysis of hematopoietic populations representing all lineages revealed that mRNA levels of *Pon2* were low or undetectable during early B cell development. In contrast, Ph^+ B-ALL samples were marked by a sharp peak of *PON2* expression (Fig. 1*B*). Consistent with these observations, PON2 protein levels were elevated in patient-derived B-ALL cells compared to normal cord blood $CD19^+$ B cells (Fig. 1*C*). These findings prompted us to examine whether *PON2* expression levels are predictive of poor or favorable outcomes in B-ALL. In two clinical B-ALL cohorts for the adult B-ALL ECOG E2993 trial, higher than median *PON2* mRNA levels were associated with shorter overall survival (OS) ($P = 0.02$, Fig. 1*D*; $P = 0.003$, Fig. 1*E*), suggesting that high *PON2* expression may affect the course of disease in adult B-ALL.

Notably, higher than median *PON2* mRNA levels were associated with unfavorable outcomes for both OS ($P = 0.001$; Fig. 1*F*) and relapse-free survival (RFS; $P = 1.1E\text{-}5$; Fig. 1*G*) in pediatric high-risk B-ALL (COG P9906). Furthermore, a multivariate analysis revealed that high *PON2* mRNA levels represent an independent risk factor and predicted poor patient outcome independently from established risk factors, e.g., *IKZF1* deletion ($P = 3.3E\text{-}6$ for OS, Fig. 1*H* and *SI Appendix*, Table S1; $P = 6.1E\text{-}7$ for RFS, Fig. 1*I* and *SI Appendix*, Table S2). In addition, *PON2* mRNA levels were associated with positive minimal residual disease (MRD^+) status in B-ALL patients following initial treatment ($P = 0.001$; Fig. 1*J*). Comparing matched patient samples from 29 B-ALL patients at the time of diagnosis and subsequent relapse revealed on average higher *PON2* mRNA levels at the time of relapse ($P = 0.041$; Fig. 1*K*). Taken together, high expression levels of *PON2* predict poor clinical outcomes in both pediatric and adult B-ALL. In contrast, *PON2* expression levels were not associated with clinical outcomes for mature B cell lymphomas and multiple myeloma (*SI Appendix*, Fig. S1 *B–E*), suggesting a unique, perhaps stage-specific, connection between PON2 and B-ALL.

Pon2 Is Required for Survival and Proliferation of Both Human and Murine B-ALL Cells but Not Normal B Cell Development. To elucidate a role of PON2 in B-ALL, we modeled *Pon2* deficiency in two mouse models for B-ALL driven by the oncogenic *BCR-ABL1* tyrosine kinase or $NRAS^{G12D}$ (25; Fig. 2). Loss of *Pon2* markedly slowed proliferation of both *BCR-ABL1*- and $NRAS^{G12D}$-driven B-ALL cells and induced strong up-regulation of cell cycle checkpoint molecules Arf and p21 (Fig. 2 *A* and *B*). In line with these observations, *Pon2* deficiency led to $G_{0/1}$-cell cycle arrest (Fig. 2 *C* and *D*) and diminished the colony forming ability of *BCR-ABL1* and $NRAS^{G12D}$ B-ALL cells by ~10- to 25-fold, respectively (Fig. 2 *E* and *F*). Based on these findings, we tested whether Pon2 affects the course of B-ALL disease in transplant models. To this end, one million luciferase-labeled $Pon2^{+/+}$ or $Pon2^{-/-}$ *BCR-ABL1* (Fig. 2*G*)- or $NRAS^{G12D}$-driven (Fig. 2*H*) B-ALL cells were injected into sublethally irradiated NSG mice, and expansion of leukemia burden was monitored by luciferase bioimaging. *BCR-ABL1* and $NRAS^{G12D}$ B-ALL cells expressing *Pon2* rapidly expanded and developed fatal disease in transplant recipient mice (Fig. 2 *G* and *H*). In contrast, loss of *Pon2* function in *BCR-ABL1* B-ALL cells delayed onset of disease and prolonged survival of recipient mice (Fig. 2*G* and *SI Appendix*, Fig. S2*A*). Notably, only one out of six mice bearing *Pon2*-deficient $NRAS^{G12D}$ B-ALL cells developed fatal leukemia (Fig. 2*H*). The remaining mice injected with *Pon2*-deficient $NRAS^{G12D}$ B-ALL cells showed no sign of disease and were killed after 130 d for minimal residual disease studies. Unlike mice in the control group, no minimal residual disease was detected in those recipient mice (*SI Appendix*, Fig. S2*B*). Thus, our results showed that B-ALL cells critically depend on PON2 for proliferation, survival, and development of leukemia disease in vivo.

Our findings illuminated Pon2 as a previously unrecognized vulnerability in murine B-ALL cells and prompted us to study whether human B-ALL cells also depended on PON2 function. We performed CRISPR-Cas9-mediated deletion of *PON2* in pooled populations of human Ph^+ B-ALL cells (BV173; Fig. 3*A*) followed by single-cell cloning to isolate individual CRISPR-edited clones deficient in *PON2* (Fig. 3*B*). Similar to our observations made in murine B-ALL, PON2 was essential for colony forming capacity (Fig. 3 *C* and *D*) and proliferation (Fig. 3*E*), confirming the dependency of human B-ALL cells on PON2 function for proliferation and survival. Previously, using $Pon2^{-/-}$ mice, it was shown that Pon2 reduces cellular oxidative stress, attenuates inflammatory response, and modulates lipoprotein properties, thus providing a protective mechanism against atherogenesis (26). However, a potential role of Pon2 in normal B cell development has not been studied. To determine whether Pon2 function is required for malignant transformation or normal aspects of early B cell development, phenotypic analyses of bone marrow B cell populations in $Pon2^{+/+}$ and $Pon2^{-/-}$ mice were performed (25). $Pon2^{-/-}$ mice had normal numbers of pro-B and early pre-B cell subsets (Hardy fractions B-C′) (1). The late pre-B cell (Hardy fraction D; $P = 0.014$) and the immature B cell (Hardy fraction E; $P = 0.01$) subsets were only modestly decreased in $Pon2^{-/-}$ mice, and no significant phenotypic changes were observed in mature B cells (Hardy fraction F; *SI Appendix*, Fig. S2*C*). Furthermore, *Pon2* deficiency did not impact affinity maturation of germinal center B cells which retained the ability to develop antigen-specific B cells in response to immunization (*SI Appendix*, Fig. S2*D*). Hence, while Pon2 is required for leukemogenesis in B-ALL, it does not play a central role in normal B cell development.

Pon2 Facilitates Glucose Uptake and ATP Production in B-ALL Cells. Previous work demonstrated that PON2 promotes survival of lung cancer cells by counteracting mitochondrial ROS production (27). On this basis, we measured intracellular ROS production to investigate whether proliferation and survival of B-ALL cells depend on the antioxidant function of Pon2. Surprisingly, the antioxidant program in B-ALL cells is not dependent on PON2 function since ROS levels were not changed upon genetic inactivation of *Pon2* in *BCR-ABL1* and $NRAS^{G12D}$ B-ALL cells (*SI Appendix*, Fig. S3*A*). This finding suggests that Pon2 serves a different, potentially lineage-specific, function in transformed pre-B cells. Recent work by us and others highlighted a lineage-specific role of glucose transport and metabolic gatekeepers in B-ALL (4, 6, 7, 28). Beside its ability to mitigate mitochondrial ROS, recent work demonstrated that PON2 also enables glucose transport through interactions with GLUT1 (29). In B-ALL, GLUT1-dependent glucose-transport activity is a limiting factor that mediates malignant proliferation (30) and is transcriptionally repressed in normal pre-B cells by PAX5 and

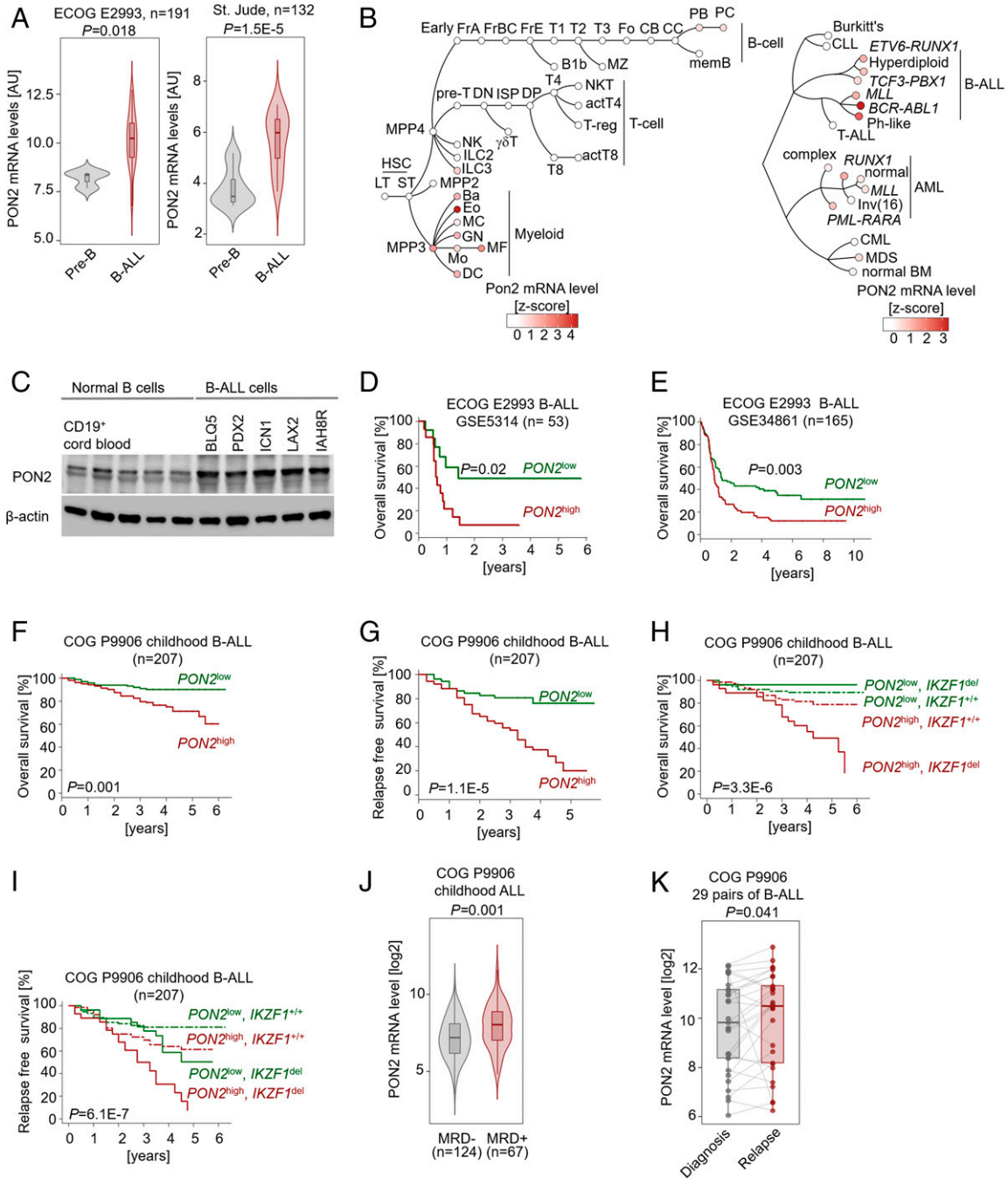

Fig. 1. High PON2 mRNA levels predict poor clinical outcome in B-ALL patients. (*A*) Gene expression data from ECOG E2993 (ALL, $n = 191$) and St. Jude (ALL, $n = 132$) clinical trials are shown. Comparison of *PON2* expression between normal pre-B cells and *Ph*$^+$ B-ALL was performed using two-tailed *t* test. (*B*) *Pon2* mRNA levels (red color scale) as determined by RNA sequencing were plotted for hematopoietic lineages (B lymphoid, T lymphoid, natural killer [NK] cell, and myeloid) as well as their differentiation stages within each lineage (GSE109125, *Left*) and for B cell malignancies, T-ALL and myeloid leukemias (GSE13159, *Right*) as dendrograms. (*C*) Western blots were performed to assess PON2 expression in B cells from healthy donors and patient-derived *Ph*$^+$ B-ALL cells. (*D* and *E*) Patients with B-ALL from the indicated cohorts of the ECOG E2993 clinical trial were segregated into two groups, *PON2*^{high} or *PON2*^{low} based on *PON2* mRNA levels (*Upper* and *Lower* quartiles in *D* and median values in *E*). OS in the two groups was assessed by Kaplan–Meier survival analysis. Imatinib-treated cases were excluded from the ECOG E2993 (GSE38461) dataset. *P* values were measured by log-rank test. (*F* and *G*) Patients in a pediatric high-risk ALL trial (Children's Oncology Group, COG P9906; $n = 207$) were segregated into two groups based on whether *PON2* mRNA levels were higher (*PON2*^{high}) or lower (*PON2*^{low}) than the median expression value. Overall survival (*F*) and relapse-free survival (*G*) were assessed in the two groups by Kaplan–Meier analysis. (*H* and *I*) Multivariate analysis of overall survival (*H*) and relapse-free survival (*I*) of pediatric B-ALL patients from the clinical trial COG P9906 ($n = 207$). Patients were segregated into four groups based on higher or lower than median expression levels of *PON2* and *IKZF1* status (*IKZF1*$^{+/+}$ or *IKZF1*^{del}; log-rank test). (*J*) MRD in B-ALL patients was assessed by flow cytometry analysis after 29 d of treatment (COG P9906). Comparison of *PON2* expression between MRD$^+$ and MRD$^-$ patients was performed using a two-sided Mann–Whitney Wilcoxon test. (*K*) Comparison of *PON2* expression between matched B-ALL samples (COG P9906) at diagnosis and relapse was performed using a two-sided Mann–Whitney Wilcoxon test.

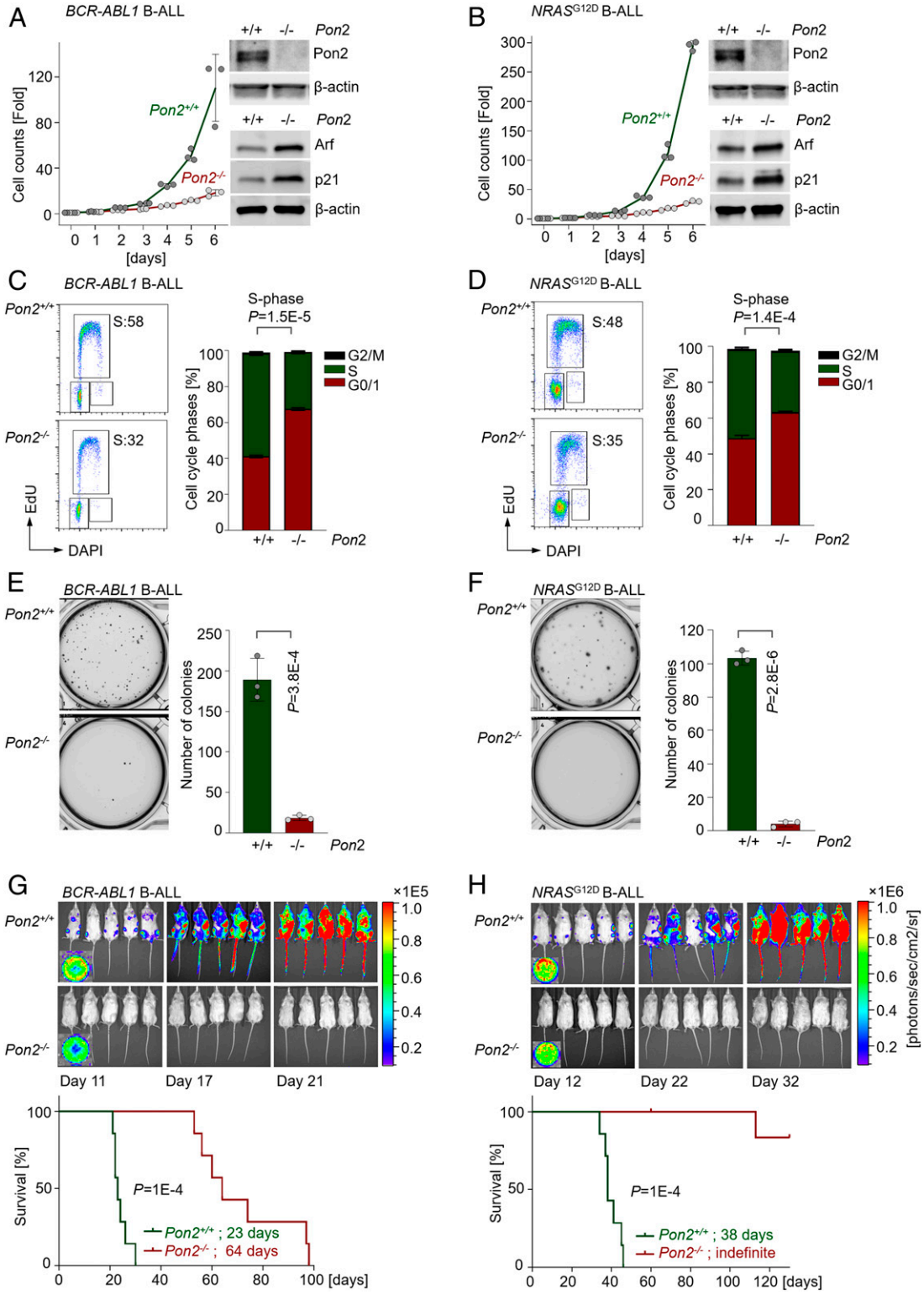

Fig. 2. Pon2 is required for survival and proliferation of BCR-ABL1- and NRAS^{G12D}-driven B cell leukemia. (*A* and *B*) Viable cell counts of *Pon2*$^{+/+}$ and *Pon2*$^{-/-}$ *BCR-ABL1* (*A*) and *NRAS*^{G12D} (*B*) B-ALL cells were measured daily for 6 consecutive days and normalized to day 0. Western blot analyses were performed to validate the deficiency of Pon2 and measure protein levels of Arf and p21 in both models. (*C* and *D*) Cell cycle analysis was performed for *Pon2*$^{+/+}$ and *Pon2*$^{-/-}$ *BCR-ABL1* (*C*) and *NRAS*^{G12D} (*D*) B-ALL cells by measuring 5-ethynyl-2′-deoxyuridine (EdU) incorporation in combination with DAPI staining. Comparison of proportions of cells in the S phase was performed using two-tailed *t* test. (*E* and *F*) Ten thousand *Pon2*$^{+/+}$ and *Pon2*$^{-/-}$ *BCR-ABL1* (*E*) and *NRAS*^{G12D} (*F*) B-ALL cells were seeded and plated in semisolid methylcellulose for colony forming assays. Colonies were counted and imaged after 10 d. *P* values were estimated using two-tailed *t* test. (*G* and *H*) One million firefly luciferase-labeled *Pon2*$^{+/+}$ or *Pon2*$^{-/-}$ *BCR-ABL1* (*G*) or *NRAS*^{G12D} B-ALL (*H*) cells were injected into each sublethally irradiated NSG mouse. Leukemia engraftment and progression were monitored by luciferase bioimaging at the indicated time points. Unit for bioimaging is photons/second/cm^2/steradian. Kaplan–Meier survival curves of the overall survival for each group (n = 7) are shown, and comparison of survival between two groups was performed by log-rank test. Data (*A*–*F*) are shown as mean ± SD (n = 3 independent experiments).

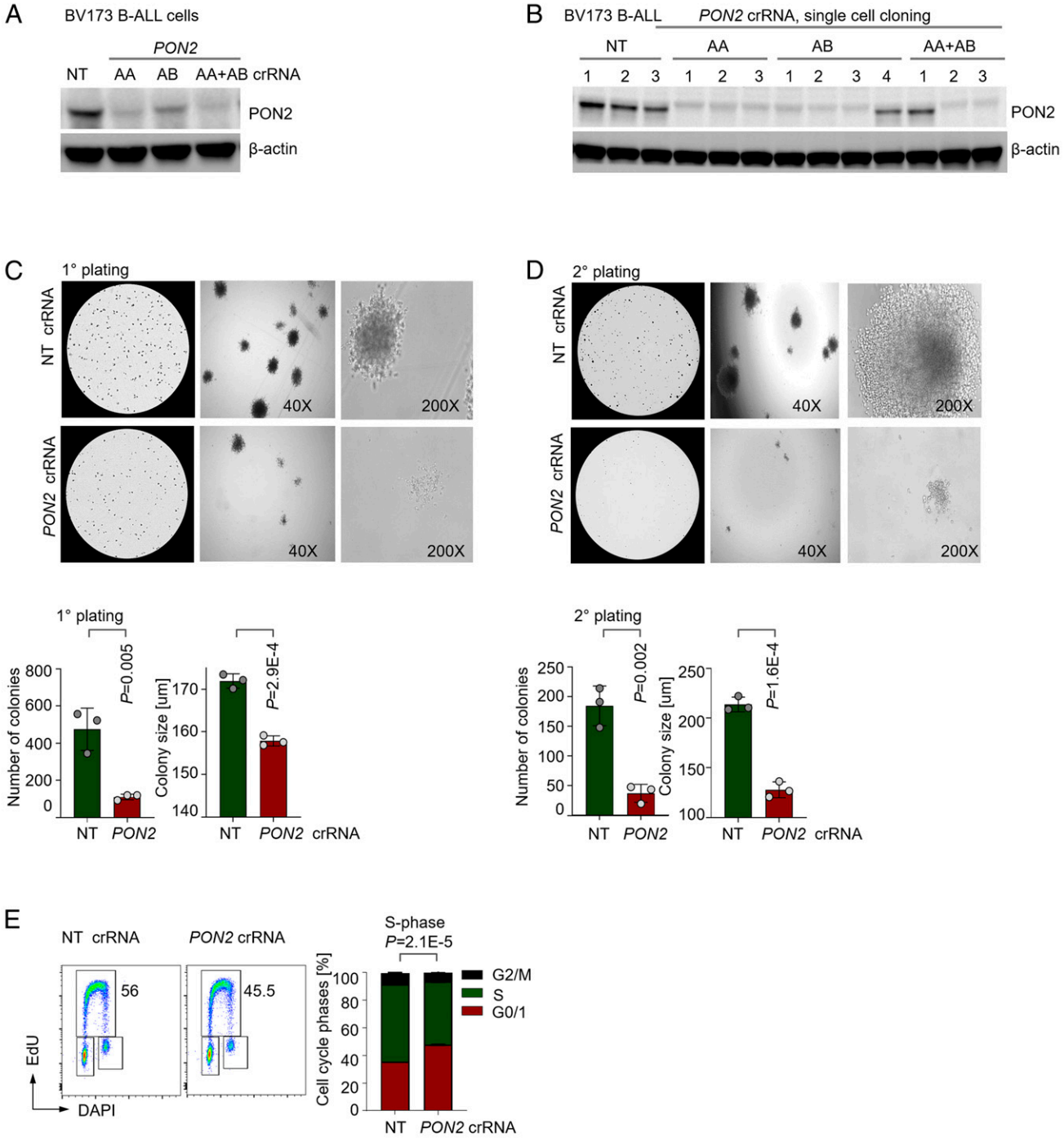

Fig. 3. CRISPR-Cas9-mediated deletion of PON2 compromises proliferation and colony formation in human Ph$^+$ B-ALL cells. (*A* and *B*) PON2 levels were assessed following CRISPR-Cas9-mediated *PON2* deletion in human *Ph*$^+$ ALL cell line (BV173) before (*A*) and after single-cell cloning (*B*). (*C* and *D*) Two thousand *PON2*$^{+/+}$ and *PON2*$^{-/-}$ B-ALL cells following single-cell cloning (*B*) were seeded and plated in semisolid methylcellulose for colony forming assays. Colonies were counted and imaged after 10 d. Representative images are shown at 40× and 200× magnification under a light microscope. Secondary plating was performed using the cells collected from primary plating. Comparison between two groups was performed for colony numbers and colony size (as measured by the diameter of each colony) using two-tailed *t* test. (*E*) Cell cycle analysis was performed for *PON2*$^{+/+}$ and *PON2*$^{-/-}$ B-ALL cells following single-cell cloning (*B*) by measuring EdU incorporation in combination with DAPI staining. Comparison of proportions of cells in the S phase was performed using two-tailed *t* test. Data are shown as mean ± SD (n = 3 independent experiments).

IKZF1 (4). For these reasons, we hypothesized that PON2 contributes to leukemogenesis in B-ALL by promoting glucose uptake to fuel increased energy demands from transforming oncogenes. Consistent with this hypothesis, glucose uptake, lactate production, and total adenosine triphosphate (ATP) levels were markedly reduced in *Pon2*-deficient *BCR-ABL1*- and *NRAS*^{G12D}-driven B-ALL cells compared to wild-type controls (Fig. 4 *A* and *B*). To further elucidate the function of Pon2 in regulating glucose and energy metabolism in B-ALL, we measured extracellular acidification rate (ECAR) under basal conditions (without glucose) and in

response to acute addition of glucose, oligomycin (inhibitor of ATP synthase), and 2-deoxyglucose (2-DG, inhibitor of glycolysis; Fig. 4*C*). Under these conditions, we compared the glycolytic responses of *Pon2*$^{+/+}$ and *Pon2*$^{-/-}$ B-ALL cells and found that Pon2 was needed to sustain glycolytic activity and enable cells to reach the maximum capacity of their glycolytic machinery (Fig. 4*C* and *SI Appendix*, Fig. S3*B*).

Given that ATP can be derived from both glycolytic and mitochondrial pathways, we also assessed mitochondrial function (oxygen consumption rate, OCR) in *Pon2*$^{+/+}$ and *Pon2*$^{-/-}$ *BCR-ABL1* B-ALL cells at the resting stage (basal respiration) and in response to acute addition of oligomycin, fluoro-carbonyl cyanide phenylhydrazone (FCCP, an electron transport chain accelerator), and a combination of rotenone and antimycin A (inhibitors of mitochondrial complexes I and III, respectively). Here bioenergetic profiles revealed that mitochondrial function was independent of PON2 in B-ALL cells (Fig. 4*D*). Collectively, these results suggest that reduced intracellular ATP levels upon loss of *Pon2* function in B-ALL were, to a significant extent, attributable to impaired glycolytic activity (Fig. 4 *A* and *B*) rather than defects in mitochondrial function.

In addition to loss-of-function studies, we examined the consequences of gain-of-function of Pon2 in B-ALL cells by using a doxycycline (Dox)-inducible Tet-on Pon2 vector system. Inducible overexpression of Pon2 augmented intracellular ATP levels in *Pon2*$^{+/+}$ B-ALL cells (Fig. 4*E*). Likewise, reconstitution of *Pon2* expression increased ATP levels in *Pon2*$^{-/-}$ B-ALL cells (Fig. 4 *E* and *F*). Notably, a point mutation that specifically abrogates Pon2 lactonase activity (Pon2^{H114Q}) (17) retained intracellular ATP levels (*SI Appendix*, Fig. S3 *C* and *D*), suggesting that the effect of Pon2 on glucose transport and energy metabolism is independent from its lactonase activity. While intracellular ATP levels were not affected by loss of lactonase activity, other aspects of PON2-dependent survival may require a functional lactonase moiety.

We next validated the role of PON2 in glucose uptake and ATP production in human *Ph*$^{+}$ B-ALL cells and examined the impact of CRISPR-Cas9-mediated deletion of *PON2*. To achieve complete biallelic deletion of *PON2* in human *Ph*$^{+}$ B-ALL cells, CRISPR-Cas9-mediated deletion of *PON2* in bulk populations was followed by single-cell cloning and expansion of outgrowth from single cells. Glucose uptake and intracellular ATP levels were assessed in individual CRISPR-edited *PON2*-deficient clones isolated from single-cell cloning (Figs. 3*B* and 4*G*). Confirming results obtained with mouse *Pon2*$^{-/-}$ B-ALL cells, *PON2* deficiency curtailed glucose uptake and total ATP levels (Fig. 4*G*). While genetic defects in the metabolic gatekeepers *PAX5* and *IKZF1* occur in over 80% of B-ALL cases (4), we here identified PON2, independent of its lactonase function, as an alternative mechanism to elevate glucose uptake and ATP production to promote leukemogenesis in B-ALL.

A Rationale for Targeting PON2 in Combination with Glucocorticoids. Glucocorticoids (GCs) have a central role in the majority of chemotherapy regimens for B-ALL (31). GCs, including dexamethasone (Dex), act through the nuclear hormone receptor NR3C1 and were shown to inhibit the glucose transport system (32). Resistance to GCs is often acquired in B-ALL patients, for instance through NR3C1 mutations, and represents a serious complication in the treatment of patients with B-ALL (33). Previously, we showed that PAX5 and IKZF1 exert their metabolic gatekeeper functions not only through repression of glucose uptake (e.g., *GLUT1*) but also through transcriptional activation of *NR3C1* (4). Given that our results here suggest that PON2 opposes metabolic gatekeeper functions by enabling glucose transport (Fig. 4), we tested the interactions between *PON2* deficiency and Dex treatment in eradicating B-ALL cells. Loss of *Pon2* function potentiated the effects of Dex in mouse *BCR-ABL1* (half maximal inhibitory concentration [IC_{50}]: 269 nM for *Pon2*$^{+/+}$; IC_{50}: 61 nM for *Pon2*$^{-/-}$)- and *NRAS*^{G12D} (IC_{50}: 481 nM for *Pon2*$^{+/+}$; IC_{50}: 177 nM for *Pon2*$^{-/-}$)-driven B-ALL cells (Fig. 4*H*). Likewise, genetic ablation of *PON2* in human *Ph*$^{+}$ B-ALL cells substantially shifted the dose–response curve for Dex treatment (IC_{50} > 4 μM for nontargeting [NT] crRNA; IC_{50}: 1.6 μM for *PON2* crRNA), demonstrating that *PON2* deficiency sensitizes B-ALL cells to Dex (Fig. 4*H*).

PON2 Promotes Glucose Transport by Blocking the Interaction between GLUT1 and STOM. Glucose uptake and flux through the proximal portion of the glycolysis pathway is mediated by the PI3K/AKT pathway (34). AKT induces glucose uptake by increasing expression of *GLUT1* and stimulating the translocation of GLUT4 and GLUT1 to the cell surface (35, 36). In addition, oncogenic RAF/MEK/ERK signaling promotes glycolysis through regulation of GLUT1 and GLUT3 (37). Thus, we tested whether activation of AKT and ERK may be involved in PON2-dependent glucose uptake and ATP production. Western blot analysis showed that *Pon2* deficiency had no effects on Akt phosphorylation in both *BCR-ABL1*- and *NRAS*^{G12D}-driven B-ALL cells (*SI Appendix*, Fig. S3*E*). Similarly, phosphorylation of Erk remained largely unchanged upon genetic ablation of *Pon2* in *NRAS*^{G12D} B-ALL cells (*SI Appendix*, Fig. S3*E*). We conclude that impaired glucose uptake and ATP production observed in *Pon2*$^{-/-}$ B-ALL cells were caused by other mechanisms rather than changes in Akt and Erk activity.

The integral membrane protein stomatin (STOM) (38) associates with GLUT1 and inhibits its glucose-transport activity (39, 40). Similar to the gene expression profile of *Pon2* (Fig. 1*B*), *Stom* expression levels were low during early B cell development (*SI Appendix*, Fig. S1*F*). This finding suggests that PON2 and STOM regulate glucose uptake at a low setpoint in normal cells, whereas expression levels of both proteins is much higher in transformed B-ALL cells. Interestingly, coimmunoprecipitation (co-IP) assays revealed that PON2 interacts with GLUT1 and STOM in human B-ALL cells (Fig. 5*A*). While interpretation on the basis of PON2 overexpression is limited, this finding suggests that PON2 promotes glucose transport by blocking the interaction between GLUT1 and STOM in B-ALL cells. We performed CRISPR-Cas9-mediated deletion of *STOM* in *PON2*$^{+/+}$ and *PON2*$^{-/-}$ human B-ALL cells followed by single-cell cloning to isolate individual clones deficient in *STOM* (Fig. 5*B* and *SI Appendix*, Fig. S3 *F* and *G*). To study the consequences of genetic ablation of *STOM* on glucose transport in B-ALL, we assessed glucose uptake using two different approaches: 1) the amounts of glucose consumed from cell culture medium were measured; and 2) we determined glucose uptake using a fluorescent deoxyglucose analog, 2-NBDG (Fig. 5*B*). In the presence of PON2 expression, deletion of *STOM* alone did not significantly affect glucose transport in B-ALL cells. Conversely, loss of *PON2* function in B-ALL cells impaired glucose transport, which was fully restored upon *STOM* deletion (Fig. 5*B*). These findings suggest that expression of PON2 at high levels in B-ALL cells largely relieved STOM-mediated suppression of glucose uptake; hence STOM deletion had only minimal effects. However, in the absence of PON2, STOM was unopposed and caused profound repression of glucose uptake. In line with this scenario, we studied endogenous PON2/STOM/GLUT1 interactions and found that genetic inactivation of *PON2* markedly augmented interaction between STOM and GLUT1 in B-ALL cells (Fig. 5*C*). While previous studies demonstrated metabolic gatekeeper functions at the level of transcriptional regulation (e.g., transcriptional repression of *GLUT1* by IKZF1 and PAX5), our findings here demonstrated an additional layer of regulation at the level of protein–protein interactions. Of note, while glucose uptake was completely rescued by *STOM* deletion in *PON2*$^{-/-}$ B-ALL cells (Fig. 5*B*), intracellular ATP levels were only partially restored

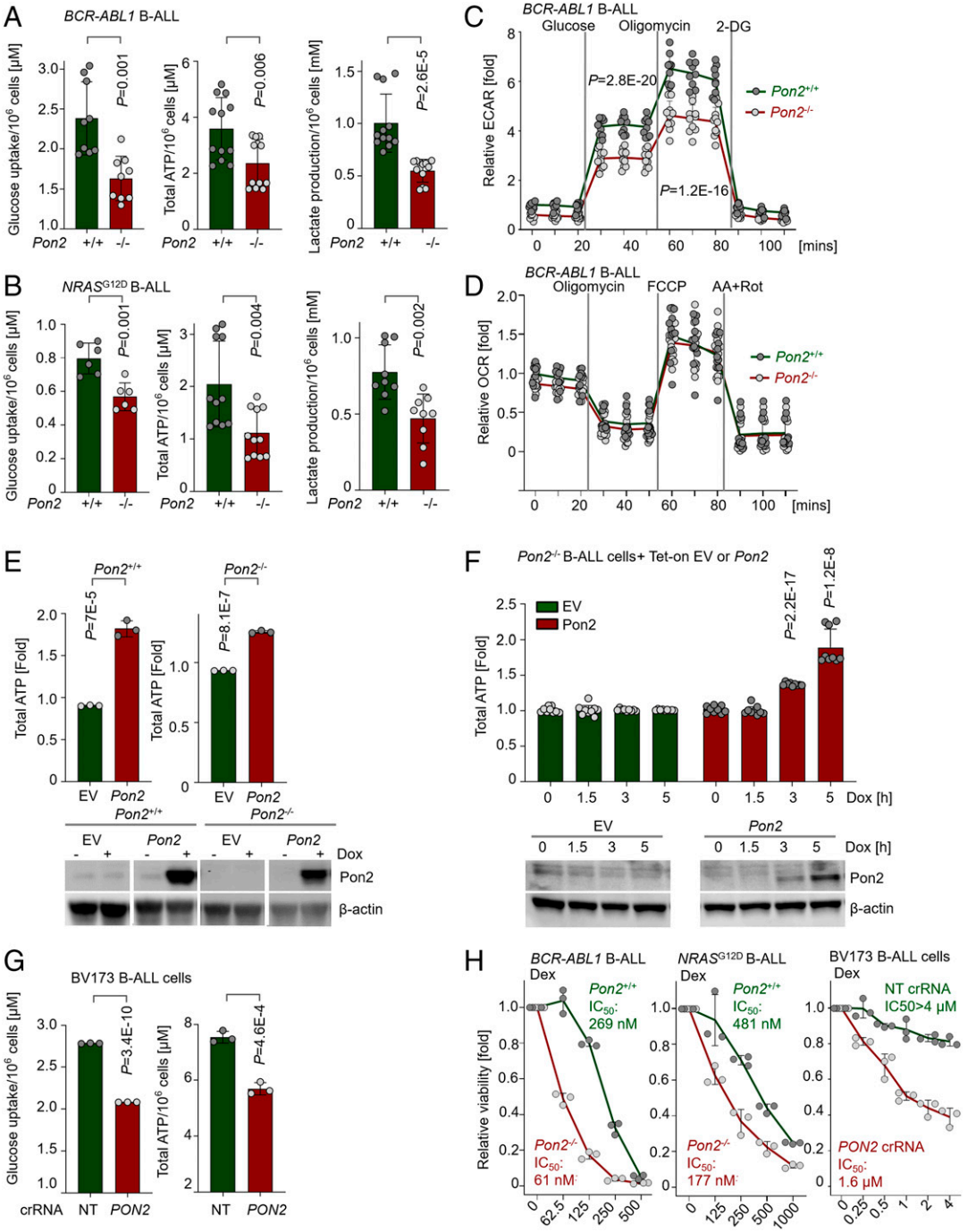

Fig. 4. Pon2 facilitates glucose uptake and ATP production in B-ALL cells. (*A* and *B*) Glucose uptake, total ATP, and lactate levels were measured for mouse *BCR-ABL1* (*A*) or *NRAS*^{G12D} (*B*) B-ALL cells. All the values were normalized to viable cell counts. *P* values were determined using two-tailed *t* test (two to three independent experiments using biological replicates, each done with technical triplicate). (*C*) ECARs and (*D*) OCRs were measured in *Pon2*$^{+/+}$ or *Pon2*$^{-/-}$ *BCR-ABL1* B-ALL in response to various treatments as indicated in the figure. AA plus Rot: antimycin A and rotenone. Data shown as mean ± SD, summarizing results obtained using two to three biological replicates (two for *C* and three for *D*), each done with three or more technical replicates. (*E*) *Pon2*$^{+/+}$ or *Pon2*$^{-/-}$ mouse *BCR-ABL1* B-ALL cells were transduced with doxycycline-inducible *Pon2* or EV control. Total ATP levels and Pon2 protein levels were measured upon 24 h of doxycycline (1 μg/mL) treatment. ATP levels in each sample were first normalized to viable cell counts and then normalized to the corresponding nondoxycycline-treated control, and comparison between *Pon2*-overexpressing and empty vector groups was performed using two-tailed *t* test. (*F*) Total ATP levels and Pon2 protein levels were measured at indicated time points upon doxycycline treatment. ATP levels were first normalized to viable cell counts and then normalized to empty vector controls; and comparison between *Pon2*-overexpressing and empty vector groups was performed using two-tailed *t* test (three independent experiments performed on separate days, each done with technical triplicate). (*G*) Glucose uptake and total ATP levels were measured in *PON2*$^{+/+}$ or *PON2*$^{-/-}$ BV173 cells and normalized to viable cell counts. Comparison between two groups was performed using two-tailed *t* test. (*H*) *Pon2*$^{+/+}$ or *Pon2*$^{-/-}$ mouse *BCR-ABL1* or *NRAS*^{G12D} B-ALL, or human *Ph*$^{+}$ B-ALL (BV173) cells were treated with increasing concentrations of dexamethasone (72 h). Cell viability was determined and normalized to the vehicle-treated group. IC_{50} values were determined using the CompuSyn software based on average effect value at each dose. Data are shown as mean ± SD (n = 3).

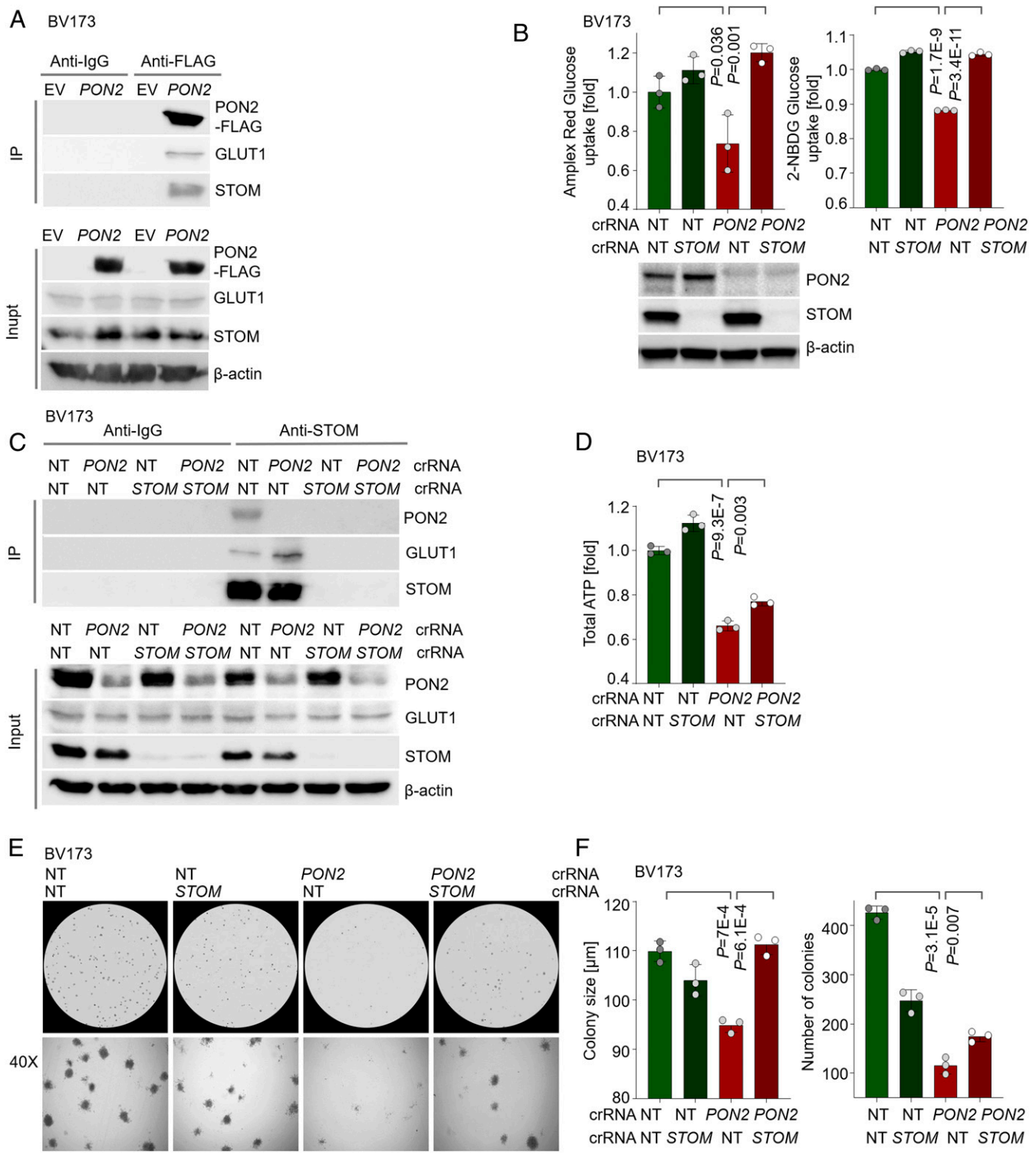

Fig. 5. PON2 promotes glucose uptake via interfering with GLUT1-STOM interaction. (*A*) Coimmunoprecipitation assay was performed in BV173 cells expressing empty vector or FLAG-tagged *PON2* using either IgG or anti-FLAG antibody. Immunoprecipitates and lysates were analyzed by Western blotting. (*B*) PON2 and STOM levels in BV173 cells were assessed following CRISPR-Cas9-mediated gene deletion and subsequent single-cell cloning. Glucose uptake was measured using the Amplex Red Glucose Assay Kit (*Left*), and 2-NBDG staining (*Right*), respectively. Median fluorescence intensity (MFI) of 2-NBDG staining was determined to compare the glucose uptake level among different groups. (*C*) Coimmunoprecipitation assay was performed to study endogenous PON2/STOM/GLUT1 interactions in BV173 cells expressing *PON2* or in CRISPR-Cas9-edited BV173 cells deficient in *PON2*, with or without *STOM* deletion, using either IgG or anti-STOM antibody. Immunoprecipitates and lysates were analyzed by Western blotting. (*D*) Total ATP levels were measured. All the data were first normalized to viable cell counts and then normalized to $PON2^{+/+}$ $STOM^{+/+}$ BV173 cells. *P* values were determined using one-way ANOVA and Turkey's multiple comparison test. (*E* and *F*) Two thousand BV173 cells with the indicated genotypes were seeded and plated in semisolid methylcellulose for colony forming assays. Colonies were imaged following 10 d (*E*). Representative images are shown at 40× magnification. *P* values were calculated for comparison of colony numbers and colony size using two-tailed *t* test with multiple test correction (*F*). Data are shown as mean ± SD ($n = 3$).

(Fig. 5*D*). Nonetheless, functional colony forming assays revealed that deletion of *STOM* in *PON2*$^{-/-}$ B-ALL cells largely restored the number and size of B-ALL colonies (Fig. 5 *E* and *F*). Therefore, PON2, at least in part, mediates proliferation and survival of B-ALL cells by blocking the interaction between GLUT1 and STOM to facilitate glucose transport. A previous study showed that PON2 regulates GLUT1-mediated glucose transport in a similar manner in pancreatic cancer cells (29). Interestingly, in line with our observations (*SI Appendix*, Fig. S3*A*), no change in intracellular ROS levels was observed upon *PON2* ablation in pancreatic cancer cells (29). While PON2 promotes survival of solid tumor cells (e.g., lung cancer) by balancing mitochondrial redox homeostasis (27), our results collectively indicate that PON2 enables B cell transformation by subverting metabolic gatekeeper functions. Hence, PON2 likely promotes tumorigenesis in a cell type-specific manner.

PON2 Lactonase Activity Can Be Leveraged as Synthetic Lethality in B-ALL Cells. Thus far, we have demonstrated a critical role of PON2 in enabling glucose transport in B-ALL cells, which is independent of its lactonase function. The bacterial signaling molecule lactone-3OC12 is rapidly hydrolyzed by PON2 to a cytotoxic intermediate 3OC12 acid which, unlike the lactone prodrug, accumulates in cells and leads to intracellular acidification (17) (*SI Appendix*, Fig. S1*A*) and caspase 3/7-dependent apoptosis (18). On this basis, we studied here whether the lactonase activity of PON2 can be leveraged in a prodrug-based strategy to kill B-ALL cells that aberrantly express PON2 at high levels. We examined the cytotoxic effects of the lactone-prodrug 3OC12 on a panel of patient-derived B-ALL cells as well as lymphoma cell lines and studied their correlation with mRNA expression levels of *PON2* (*SI Appendix*, Fig. S4 *A* and *B*). Notably, we observed a positive correlation ($r = 0.95$; $P < 1E\text{-}4$) between growth inhibition and expression levels of *PON2*. For instances, B-ALL cells with the highest mRNA levels of *PON2* (e.g., LAX2 and PDX2) exhibited the most substantial inhibition in cell viability. Conversely, mature B cell lymphoma cell lines expressing low mRNA levels of *PON2* were highly resistant to 3OC12 (*SI Appendix*, Fig. S4 *A* and *B*). Similar results were obtained when we compared the protein levels of patient-derived B-ALL samples (*PON2*^{high}; 3OC12 sensitive) and human mature B cell lymphoma cells (*PON2*^{low}; 3OC12 resistant) with their dose–response curves upon 3OC12 treatment (*SI Appendix*, Fig. S4*C*). Together, these findings suggest that expression levels of *PON2* are predictive of responses to 3OC12 in B cell malignancies.

To test a potential causative link between aberrant PON2 expression in B-ALL cells and selective sensitivity to 3OC12, we studied gain and loss of function of *Pon2* in mouse *BCR-ABL1* and *NRAS*^{G12D} B-ALL cells. Genetic inactivation of *Pon2* conferred resistance to 3OC12 (Fig. 6*A*) and abrogated accumulation of intracellular ROS resulting from 3OC12 treatment (Fig. 6*C*) in B-ALL cells. On the contrary, reconstitution of *Pon2* in *Pon2*$^{-/-}$ B-ALL cells partially restored sensitivity to 3OC12. Furthermore, overexpression of Pon2 substantially sensitized B-ALL cells expressing endogenous Pon2 to 3OC12 treatment (Fig. 6*B* and *SI Appendix*, Fig. S4*D*). Consistent with these observations, CRISPR-Cas9-mediated *PON2* deletion in patient-derived B-ALL cells decreased responsiveness to 3OC12, while overexpression of *PON2* increased sensitivity to 3OC12 (Fig. 6 *D* and *E* and *SI Appendix*, Fig. S4 *E–H*). In addition, 3OC12 promptly induced ROS levels in patient-derived B-ALL cells expressing high levels of PON2, but not in mature B cell lymphoma cells expressing low levels of PON2 (*SI Appendix*, Fig. S5*A*). Thus, reflecting aberrant expression of *PON2* (Fig. 1 and *SI Appendix*, Fig. S4), 3OC12 induces cytotoxic effects in B-ALL cells.

Mechanistically, we observed elevated phosphorylation of proapoptotic p38 MAPK and caspase-3 activation in patient-derived B-ALL cells, but not in mature B cell lymphoma cells, following 3OC12 treatment (*SI Appendix*, Fig. S5*B*), which did not impact endogenous PON2 expression (*SI Appendix*, Fig. S5*C*). Mirroring the central role of PON2 expression in setting the threshold for responses to 3OC12, activation of p38 phosphorylation and caspase-3 upon 3OC12 treatment was further augmented by overexpression of PON2 in patient-derived B-ALL cells (Fig. 6*F*). To complement our in vitro observations in a proof-of-concept transplant experiment, we first confirmed that our target dose level of 25 mg/kg 3OC12 was well tolerated in transplant recipient mice (Fig. 6*G*). Luciferase-labeled patient-derived B-ALL cells were injected into sublethally irradiated NSG mice, which were treated with intraperitoneal injections of vehicle or 25 mg/kg 3OC12. In vivo expansion of leukemic cells was monitored by luciferase bioimaging. B-ALL cells readily expanded in transplant recipient mice treated with vehicle control as shown by bioimaging (Fig. 6*H*). In contrast, 3OC12 treatment delayed the onset of fatal disease and prolonged overall survival of recipient mice (P = 6E-4; Fig. 6*I*). In summary, our findings highlight the critical role of PON2 in B-ALL leukemogenesis in large part because of its role as an alternative mechanism to enable glucose transport to subvert the metabolic gatekeepers and provide a rationale for leveraging its lactonase activity as synthetic lethality to overcome drug resistance in refractory B-ALL (Fig. 6*J*).

Discussion

B cells are marked by restrictive metabolism as they face metabolic constraints on glucose and energy supply. B lymphoid transcription factors (e.g., IKZF1 and PAX5), which mediate B cell lineage commitment, repress glucose transport and energy supply, thus acting as metabolic gatekeepers. While these previous studies showed regulation of metabolic gatekeeper functions at the transcriptional level, we here discovered an additional layer of regulation based on protein–protein interactions between PON2 and STOM.

B cell precursors are defined by a state of chronic energy deficit, as reflected by their low baseline ATP levels, and restriction of mitochondrial number and volume (41). To jumpstart oncogenic signaling and enable transformation of pre-B cells, mechanisms must be in place to bypass the metabolic barrier to fuel oncogenic signaling. *PON2* expression levels are low in B cell precursors, which is consistent with intact metabolic gatekeeper functions and restricted energy supply during normal B cell development. In contrast, using genetic and metabolic analyses, we uncovered aberrant *PON2* expression in B-ALL cells as a mechanism to bypass metabolic gatekeeper functions and enable overt transformation. PON2 enables the glucose-transport activity of GLUT1 by blocking the interaction between the transporter and its inhibitor stomatin, thus increasing subsequent ATP production in B-ALL. Consistent with the central role of Pon2-mediated glucose transport, B-ALL cells critically depend on Pon2 for proliferation and survival as well as leukemia development in transplant recipient mice. The significance of glucose and energy supply in leukemogenesis is matched by observations made in the clinic: Adult B-ALL patients with hyperglycemia were less likely to achieve durable disease remission and had worse clinical outcomes compared to patients with normal glucose levels (8). Furthermore, children with obesity or type 2 diabetes mellitus with higher glucose and insulin serum levels were more likely to relapse and had worse overall outcomes (9–11). Interestingly, unlike in B-ALL, *PON2* expression levels in B cell lymphomas are not associated with clinical outcomes (*SI Appendix*, Fig. S1). This is in line with our previous observations that genetic lesions in the metabolic gatekeepers *IKZF1* and *PAX5* occur very frequently in B-ALL but are extremely rare in B cell lymphomas derived from mature B cells, and that loss of function of the energy stressor pathway LKB1/AMPK is deleterious in B-ALL cells but not in B cell lymphoma cells (4). Collectively, these findings indicate stage-specific metabolic control of glucose uptake and utilization in B-ALL and

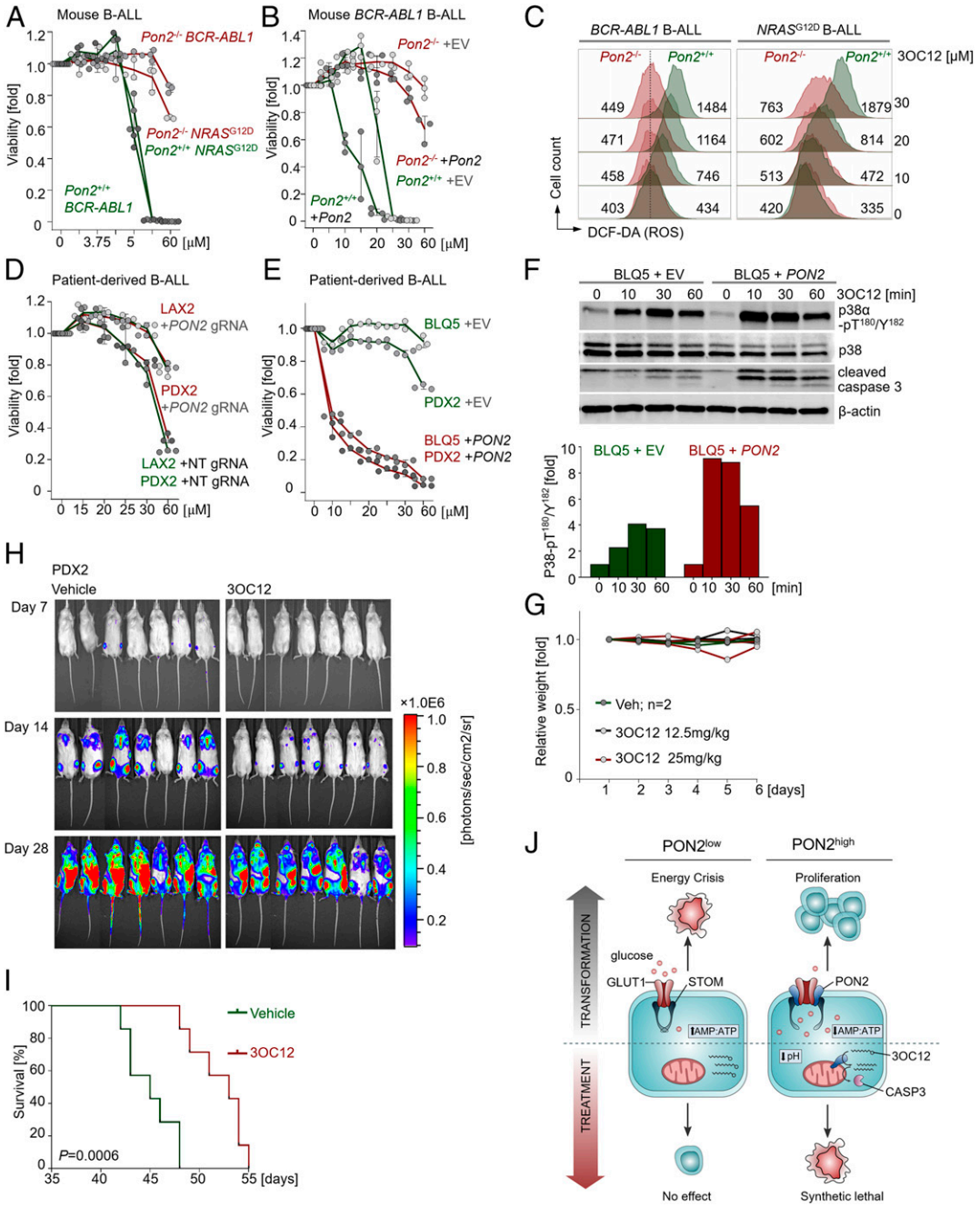

Fig. 6. PON2 lactonase activity can be leveraged in a prodrug-based strategy to kill PON2^{high} leukemia cells. (*A*) *Pon2*$^{+/+}$ or *Pon2*$^{-/-}$ *BCR-ABL1* and *NRAS*^{G12D} mouse B-ALL cells were treated with 3OC12 at the indicated concentrations for 3 d, and cell viability was determined. (*B*) *Pon2*$^{+/+}$ or *Pon2*$^{-/-}$ mouse *BCR-ABL1* B-ALL cells overexpressing *Pon2* or empty vector were treated with 3OC12 at the indicated concentrations for 3 d. Cell viability was determined. (*C*) ROS levels were measured in *Pon2*$^{+/+}$ or *Pon2*$^{-/-}$ mouse *BCR-ABL1* and *NRAS*^{G12D} B-ALL cells after 2 h of 3OC12 treatment. (*D* and *E*) Patient-derived *Ph*$^{+}$ B-ALL cells (LAX2 and PDX2) expressing gRNAs targeting *PON2* or nontargeting (NT) gRNAs were treated with 3OC12 at the indicated concentrations for 3 d. (*D*) From top to bottom: LAX2 +*PON2* gRNA, PDX2 +*PON2* gRNA, LAX2 +NT gRNA, PDX2 +NT gRNA. Patient-derived *Ph*$^{+}$ B-ALL cells (BLQ5 and PDX2) expressing *PON2* or empty vector were treated with 3OC12 at the indicated concentrations for 3 d (*E*). Cell viability was determined. (*F*) Western blotting was performed to measure the levels of phospho-p38-pT^{180}/Y^{182}, total p38, and cleaved caspase-3 in 3OC12-treated patient-derived *Ph*$^{+}$ B-ALL cells (BLQ5) with or without *PON2* overexpression. The bands of phospho-p38-pT^{180}/Y^{182} were quantified using ImageJ, and intensities were first normalized to those of total p38 and β-actin, and then normalized to values obtained from time 0 to determine the fold change. (*G*) NSG mice treated with 3OC12 or vehicle were weighed for 6 d consecutively. Weight measurements are shown (vehicle, $n = 2$; 3OC12, 12.5 mg/kg, $n = 3$; 3OC12, 25 mg/kg, $n = 3$). Each line represents measurement from one mouse. (*H* and *I*) Half a million luciferase-labeled PDX2 cells were injected via tail vein into each sublethally irradiated (2.5 Gy) NSG mouse. Prior to injection, cells were pretreated with vehicle or 3OC12 (100 μM) for 1 h and resuspended in PBS following washout of the vehicle or the lactone prodrug. Recipient mice were intraperitoneally injected with vehicle or 25 mg/kg of 3OC12 for 7 consecutive days. Leukemia engraftment and progression were monitored by luciferase bioimaging at the indicated time points (*H*). Kaplan–Meier survival curves of the overall survival for each group ($n = 7$) are shown, and comparisons of survival between two groups were performed by log-rank test (*I*). (*J*) PON2 enables glucose uptake and energy production by blocking the interaction between GLUT1 and its inhibitor STOM, thereby mitigating energy crisis caused by the metabolic gatekeepers and promoting leukemogenesis in B-ALL. While not required for glucose uptake, the lactonase activity of PON2 to hydrolyze the lactone-prodrug 3OC12 to 3OC12 acid, which induces intracellular acidification, caspase-3 activation, and subsequent cell death, can be exploited for eradicating B-ALL cells.

mature B cell lymphoma and support the role of PON2 as a specific metabolic vulnerability in B-ALL. Interestingly, our findings also established a rationale for leveraging the lactonase function of PON2 to eradicate B-ALL cells and overcome drug resistance in refractory B-ALL. Hence, the lactonase activity of PON2, while not required for energy production to support proliferation and survival (*SI Appendix*, Fig. S3 *C* and *D*), could be engaged as a previously unrecognized synthetic lethality to overcome drug resistance in B-ALL cells.

Materials and Methods

Human Blood and Patient-Derived B-ALL Samples. Patient-derived B-ALL samples were collected in compliance with the Institutional Review Board of the University of California, San Francisco and the City of Hope Comprehensive Cancer Center (*SI Appendix*, Table S3). The samples were deidentified prior to use in our study. The cells were cultured as described in *SI Appendix*, *Supplemental Materials and Methods*.

Cell Lines. The human cell lines were purchased from DSMZ or ATCC (*SI Appendix*, Table S4) and maintained in Roswell Park Memorial Institute medium (RPMI-1640; Invitrogen) with GlutaMAX containing 10 to 20% fetal bovine serum (FBS), 100 IU/mL penicillin, and 100 μg/mL streptomycin. Cell cultures were kept at 37 °C in a humidified incubator with 5% CO_2. All cell lines were tested to be mycoplasma-free before experimental usage (MycoAlertPLUS, LONZA).

Genetic Mouse Models. All the genetic mouse models used in this study are listed in *SI Appendix*, Table S5. *Pon2*$^{-/-}$ mice (26) were backcrossed to wild-type C57BL/6J for more than eight generations. Wild-type C57BL/6J and NOD.Cg-*Prkdc*^{scid} *Il2rg*^{tm1Wjl}/SzJ, B6.129S2-*Ighm*^{tm1Cgn}/J mice were purchased from The Jackson Laboratory. For animals bred in house, littermates of the same gender were randomly assigned to experimental groups. All mouse experiments were subject to institutional approval by the University of California, San Francisco and the Comprehensive Cancer Center of City of Hope Animal Care and Use Committee.

Murine Primary and Leukemia Cells. Bone marrow and splenic cells were harvested from female mice between 6 and 10 wk of age as previously described (25). A detailed description is included in *SI Appendix*, *Supplemental Materials and Methods*.

Retroviral and Lentiviral Transduction. Constructs used for retroviral or lentiviral transduction are listed in *SI Appendix*, Table S6 and were generated as previously described (25). A detailed description is given in *SI Appendix*, *Supplemental Materials and Methods*.

Colony Forming Assay for Murine ALL Cells. Ten thousand *Pon2*$^{+/+}$ and *Pon2*$^{-/-}$ *BCR-ABL1* and *NRAS*^{G12D} B-ALL cells were seeded and plated on semisolid methylcellulose for colony forming assays. Colonies were counted and imaged following 10 d. See *SI Appendix*, *Supplemental Materials and Methods* for a detailed description.

In Vivo Leukemia Cell Transplantation. *Pon2*$^{+/+}$ or *Pon2*$^{-/-}$ *BCR–ABL1* or *NRAS*^{G12D} B-ALL cells were labeled with retroviral firefly luciferase and selected by blasticidin (20 μg/mL) and then injected into sublethally irradiated (200 cGy) NSG mice via the tail vein. Eight- to 10-wk-old female NSG mice were randomly assigned to different groups before injection. A mouse was killed when it presented signs of leukemia burden such as weight loss, a back hunched, and inability to move. Bone marrow and spleen cells were harvested and analyzed by flow cytometry to examine leukemia infiltration. Kaplan–Meier survival curves were drawn to show the overall survival for each group, and the comparison of survival between two groups was performed by the log-rank test. All the mouse-related experiments were approved by the Beckman Research Institute of City of Hope Animal Care and Use Committee.

Assessment of C12 Efficacy In Vivo. Patient-derived *BCR-ABL1* ALL cells (PDX2) were labeled with firefly luciferase and selected by blasticidin (20 μg/mL). Cells were preloaded with 3OC12 (100 μM; Sigma-Aldrich; Cat. #09139) or vehicle for 1 h and then resuspended in phosphate-buffered saline (PBS) after washing out of the vehicle or drug. Half a million cells were injected into sublethally irradiated (250 cGy) NSG recipient mice via the tail vein. Eight- to 10-wk-old female NSG mice (The Jackson Laboratory) were randomly assigned to each group before injection. Recipient mice were treated with vehicle or 3OC12 (25 mg/kg) via intraperitoneal injections for 7 consecutive days. The in vivo expansion of leukemia cells was monitored by luciferase bioimaging (IVIS 100 bioluminescence/optical imaging system; Xenogen) at the indicated time points. Briefly, D-luciferin (Promega) was dissolved in PBS and injected intraperitoneally at a dose of 2.5 mg per mouse 15 min before measuring luminescence. All mice were anesthetized by inhaled isoflurane (5%) during the detection of light emission. A mouse was killed when it presented signs of leukemia burden such as weight loss, a hunched back, and inability to move. Kaplan–Meier survival curves were drawn to show the overall survival for each group, and the comparison of survival between two groups was performed by log-rank test.

Hapten 4-hydroxy-3-nitrophenyl acetyl (NP) Immunization Assay. Spleens from four pairs of 8- to 9-wk-old female *Pon2*$^{+/+}$ or *Pon2*$^{-/-}$ mice were harvested, and mature B cells were enriched by MojoSort Mouse Pan B Cell Isolation Kit II (Biolegend, Cat. #480088). Ten million cells were transplanted to each mature B cell-deficient mouse (B6.129S2-*Ighm*^{tm1Cgn}/J, μMT) via tail vein injection on day 0 and day 15. Eight- to 10-wk-old female μMT mice were randomly assigned to different groups before injection. Eleven recipient mice were transplanted for each group (*Pon2*$^{+/+}$→ μMT, *Pon2*$^{-/-}$ → μMT). One mouse from the *Pon2*$^{+/+}$ B cell-transplanted group was killed to check engraftment efficiency. Hapten 4-hydroxy-3-nitrophenyl acetyl (NP) conjugated to keyhole limpet haemocyanin (KLH) (NP-KLH) (Biosearch Technologies, Cat. #N-5060-25) mixed with adjuvant (Sigma-Aldrich, Cat. #S6322) ($n = 6$ for *Pon2*$^{+/+}$→ μMT, $n = 7$ for *Pon2*$^{-/-}$ → μMT) or adjuvant alone ($n = 4$ for each group) was intraperitoneally injected to recipient mice on day 19 and day 26. Recipient mice were killed on day 31, and flow cytometry was performed on splenic cells. Surface expression of CD19 and B220 was measured to validate the engraftment of donor cells in the recipient mice's spleen. CD95, GL-7, and NP-antigen levels (NP-PE [phycoerythrin]; Cat. #N-5070-1) were measured to identify the NP-responsive germinal center B cells. Anti-GL7 (BD Biosciences, Cat. #561529) were diluted 1:200, and NP-antigen and the rest of the antibodies were diluted 1:100.

CRISPR-Cas9-Mediated Gene Deletion. Patient-derived xenografts (PDXs) were sequentially transduced with two plasmids for inducible Cas9 expression by lentiviral transduction as previously described (25). A detailed description is provided in *SI Appendix*, *Supplemental Materials and Methods*.

Gene Deletion by Nonviral Genome Targeting. CrRNAs and tracrRNAs were chemically synthesized and dissolved in Nuclease-Free Duplex buffer. Equal volumes (2.3 μL) of crRNAs (100 μM) and tracrRNAs (100 μM) were mixed and denatured by incubation at 95 °C for 5 min and then annealed at room temperature. Recombinantly produced Cas9 Nuclease V3 (10 mg/mL, 9.7 μL) was then mixed with gRNA to generate RNA ribonucleoprotein (RNP) complexes. RNPs were freshly complexed before electroporation. Electroporation was performed using the Neon Transfection System (Thermo Fisher) under 1,600 v for three pulses and 10 ms per pulse. Predesigned Alt-R CRISPR-Cas9 guide RNAs and nontargeting control guide RNAs were purchased from IDT and are listed in *SI Appendix*, Table S7. To generate homogenous cell populations with identical genotype, we performed a single-cell sorting and further expanded each single cell in separate wells of 96-well plates.

Data Availability. The GEO accession number for the gene expression profile from ECOG E2993 (191 B-cell acute lymphoblastic leukemia, B-ALL, and normal samples) is GSE34861. The GEO accession number for RNAseq data for immunocyte populations representing all lineages and several differentiation stages is GSE109125. Additional accession numbers for gene expression data used in this study include: GSE13159 (2096 blood or bone marrow samples of acute and chronic leukemia patients), GSE11877 (COG P9906, 207 B-ALL), GSE5314 (ECOG E2993, 54 ALL), GSE28460 (COG P9906, 29 paired B-ALL samples), GSE10846 (diffuse large B cell lymphoma, DLBCL), GSE22762 (chronic lymphocytic leukemia, CLL), and GSE9782 (multiple myeloma, MM). Gene expression data for follicular cell lymphoma were obtained from the Lymphoma/Leukemia Molecular Profiling Project (LLMPP). Gene expression data from 132 pediatric ALL patient samples were obtained from: http://www.stjuderesearch.org/data/ALL3. All additional data are included in the article and *SI Appendix*. Further information requests and requests for reagents should be directed to and will be fulfilled by lead contact, M.M. (markus.muschen@yale.edu).

ACKNOWLEDGMENTS. We thank Lars Klemm, Franziska Auer, Anna Hecht, Janet Winchester, and current and former members of the M.M. laboratory for support and helpful discussions. The human pBABE-EV or -PON2 WT/H114Q-puro plasmids were gifts from Chi Li, University of Louisville (Louisville,

KY). Research in the M.M. laboratory is funded by the NIH/National Cancer Institute through Outstanding Investigator Award R35CA197628 (to M.M.), R01CA157644, R01CA213138, P01CA233412, the Dr. Ralph and Marian Falk Medical Research Trust Transformational Awards Program through MCG-18447-19, the Leukemia and Lymphoma Society through MCL-7000-18, and Blood Cancer Discoveries Grant BCDG-20327-20, and the Howard Hughes Medical Institute (HHMI) Grant 55108547 (to M.M.). L.P. was supported by Grants National Natural Science Foundation of China (NSFC) 81770163 and 81500139. T.S. is a Lymphoma Research Foundation Grantee. V.K. is supported by Career Development Fellow Grant 5491-20 from the Leukemia and Lymphoma Society and a Young Investigator Award from Alex's Lemonade Stand Foundation. M.M. is a HHMI Faculty Scholar.

1. M. Buchner, S. Swaminathan, Z. Chen, M. Müschen, Mechanisms of pre-B-cell receptor checkpoint control and its oncogenic subversion in acute lymphoblastic leukemia. *Immunol. Rev.* **263**, 192–209 (2015).
2. E. Papaemmanuil *et al*., RAG-mediated recombination is the predominant driver of oncogenic rearrangement in ETV6-RUNX1 acute lymphoblastic leukemia. *Nat. Genet.* **46**, 116–125 (2014).
3. S. Swaminathan *et al*., Mechanisms of clonal evolution in childhood acute lymphoblastic leukemia. *Nat. Immunol.* **16**, 766–774 (2015).
4. L. N. Chan *et al*., Metabolic gatekeeper function of B-lymphoid transcription factors. *Nature* **542**, 479–483 (2017).
5. G. Xiao *et al*., B-cell-specific diversion of glucose carbon utilization reveals a unique vulnerability in B cell malignancies. *Cell* **173**, 470–484.e18 (2018).
6. A. Martín-Lorenzo *et al*., Loss of Pax5 exploits Sca1-BCR-ABL^{p190} susceptibility to confer the metabolic shift essential for pB-ALL. *Cancer Res.* **78**, 2669–2679 (2018).
7. Z. Lu *et al*., Fasting selectively blocks development of acute lymphoblastic leukemia via leptin-receptor upregulation. *Nat. Med.* **23**, 79–90 (2017).
8. M. A. Weiser *et al*., Relation between the duration of remission and hyperglycemia during induction chemotherapy for acute lymphocytic leukemia with a hyperfractionated cyclophosphamide, vincristine, doxorubicin, and dexamethasone/methotrexate-cytarabine regimen. *Cancer* **100**, 1179–1185 (2004).
9. A. M. Butturini *et al*., Obesity and outcome in pediatric acute lymphoblastic leukemia. *J. Clin. Oncol.* **25**, 2063–2069 (2007).
10. C. B. Gelelete *et al*., Overweight as a prognostic factor in children with acute lymphoblastic leukemia. *Obesity (Silver Spring)* **19**, 1908–1911 (2011).
11. E. Orgel *et al*., Obesity is associated with residual leukemia following induction therapy for childhood B-precursor acute lymphoblastic leukemia. *Blood* **124**, 3932–3938 (2014).
12. H. Bar-Rogovsky, A. Hugenmatter, D. S. Tawfik, The evolutionary origins of detoxifying enzymes: The mammalian serum paraoxonases (PONs) relate to bacterial homoserine lactonases. *J. Biol. Chem.* **288**, 23914–23927 (2013).
13. S. Altenhöfer *et al*., One enzyme, two functions: PON2 prevents mitochondrial superoxide formation and apoptosis independent from its lactonase activity. *J. Biol. Chem.* **285**, 24398–24403 (2010).
14. A. Devarajan *et al*., Paraoxonase 2 deficiency alters mitochondrial function and exacerbates the development of atherosclerosis. *Antioxid. Redox Signal.* **14**, 341–351 (2011).
15. Y. H. Noh *et al*., Inhibition of oxidative stress by coenzyme Q10 increases mitochondrial mass and improves bioenergetic function in optic nerve head astrocytes. *Cell Death Dis.* **4**, e820 (2013).
16. H. Hagmann *et al*., Breaking the chain at the membrane: Paraoxonase 2 counteracts lipid peroxidation at the plasma membrane. *FASEB J.* **28**, 1769–1779 (2014).
17. S. Horke *et al*., Novel paraoxonase 2-dependent mechanism mediating the biological effects of the Pseudomonas aeruginosa quorum-sensing molecule N-(3-Oxo-Dodecanoyl)-L-Homoserine lactone. *Infect. Immun.* **83**, 3369–3380 (2015).
18. C. Schwarzer *et al*., Paraoxonase 2 serves a proapopotic function in mouse and human cells in response to the Pseudomonas aeruginosa quorum-sensing molecule N-(3-Oxododecanoyl)-homoserine lactone. *J. Biol. Chem.* **290**, 7247–7258 (2015).
19. M. Uhlen *et al*., A pathology atlas of the human cancer transcriptome. *Science* **357**, eaan2507 (2017).
20. H. Kang *et al*., Gene expression classifiers for relapse-free survival and minimal residual disease improve risk classification and outcome prediction in pediatric B-precursor acute lymphoblastic leukemia. *Blood* **115**, 1394–1405 (2010).
21. R. C. Harvey *et al*., Identification of novel cluster groups in pediatric high-risk B-precursor acute lymphoblastic leukemia with gene expression profiling: Correlation with genome-wide DNA copy number alterations, clinical characteristics, and outcome. *Blood* **116**, 4874–4884 (2010).
22. R. C. Harvey *et al*., Development and validation of a highly sensitive and specific gene expression classifier to prospectively screen and identify B-precursor acute lymphoblastic leukemia (ALL) patients with a philadelphia chromosome-like ("Ph-like" or "BCR-ABL1-like") signature for therapeutic targeting and clinical intervention. *Blood* **122**, 826 (2013).
23. K. G. Roberts *et al*., High frequency and poor outcome of philadelphia chromosome-like acute lymphoblastic leukemia in adults. *J. Clin. Oncol.* **35**, 394–401 (2017).
24. M. E. Ross *et al*., Classification of pediatric acute lymphoblastic leukemia by gene expression profiling. *Blood* **102**, 2951–2959 (2003).
25. J. Lee *et al*., IFITM3 functions as a PIP3 scaffold to amplify PI3K signalling in B cells. *Nature* **588**, 491–497 (2020).
26. C. J. Ng *et al*., Paraoxonase-2 deficiency aggravates atherosclerosis in mice despite lower apolipoprotein-B-containing lipoproteins: Anti-atherogenic role for paraoxonase-2. *J. Biol. Chem.* **281**, 29491–29500 (2006).
27. I. Witte *et al*., Beyond reduction of atherosclerosis: PON2 provides apoptosis resistance and stabilizes tumor cells. *Cell Death Dis.* **2**, e112 (2011).
28. M. Müschen, Metabolic gatekeepers to safeguard against autoimmunity and oncogenic B cell transformation. *Nat. Rev. Immunol.* **19**, 337–348 (2019).
29. A. Nagarajan *et al*., Paraoxonase 2 facilitates pancreatic cancer growth and metastasis by stimulating GLUT1-mediated glucose transport. *Mol. Cell* **67**, 685–701.e6 (2017).
30. T. Liu *et al*., Glucose transporter 1-mediated glucose uptake is limiting for B-cell acute lymphoblastic leukemia anabolic metabolism and resistance to apoptosis. *Cell Death Dis.* **5**, e1470 (2014).
31. G. J. Kaspers *et al*., Different cellular drug resistance profiles in childhood lymphoblastic and non-lymphoblastic leukemia: A preliminary report. *Leukemia* **8**, 1224–1229 (1994).
32. J. M. Olefsky, Effect of dexamethasone on insulin binding, glucose transport, and glucose oxidation of isolated rat adipocytes. *J. Clin. Invest.* **56**, 1499–1508 (1975).
33. C. H. Pui, W. E. Evans, Treatment of acute lymphoblastic leukemia. *N. Engl. J. Med.* **354**, 166–178 (2006).
34. M. G. Vander Heiden, L. C. Cantley, C. B. Thompson, Understanding the warburg effect: The metabolic requirements of cell proliferation. *Science* **324**, 1029–1033 (2009).
35. A. D. Kohn, S. A. Summers, M. J. Birnbaum, R. A. Roth, Expression of a constitutively active Akt Ser/Thr kinase in 3T3-L1 adipocytes stimulates glucose uptake and glucose transporter 4 translocation. *J. Biol. Chem.* **271**, 31372–31378 (1996).
36. H. L. Wieman, J. A. Wofford, J. C. Rathmell, Cytokine stimulation promotes glucose uptake via phosphatidylinositol-3 kinase/Akt regulation of Glut1 activity and trafficking. *Mol. Biol. Cell* **18**, 1437–1446 (2007).
37. T. J. Parmenter *et al*., Response of BRAF-mutant melanoma to BRAF inhibition is mediated by a network of transcriptional regulators of glycolysis. *Cancer Discov.* **4**, 423–433 (2014).
38. P. C. Havugimana *et al*., A census of human soluble protein complexes. *Cell* **150**, 1068–1081 (2012).
39. A. Montel-Hagen *et al*., Erythrocyte Glut1 triggers dehydroascorbic acid uptake in mammals unable to synthesize vitamin C. *Cell* **132**, 1039–1048 (2008).
40. J. Z. Zhang, W. Abbud, R. Prohaska, F. Ismail-Beigi, Overexpression of stomatin depresses GLUT-1 glucose transporter activity. *Am. J. Physiol. Cell Physiol.* **280**, C1277–C1283 (2001).
41. L. N. Chan, M. Müschen, B-cell identity as a metabolic barrier against malignant transformation. *Exp. Hematol.* **53**, 1–6 (2017).